

Article

Evaluating Impacts of Overloaded Heavy Vehicles on Freeway Traffic Condition by a Novel Multi-Class Traffic Flow Model

Xiang Wang * , Po Zhao and Yanyun Tao

School of Rail Transportation, Soochow University, No.8 Jixue Road, Suzhou 215000, China; pzhao@stu.suda.edu.cn (P.Z.); taoyanyun@suda.edu.cn (Y.T.)

* Correspondence: wangxiang@suda.edu.cn; Tel.: +86-0512-65158963

Received: 10 October 2018; Accepted: 5 December 2018; Published: 10 December 2018



Abstract: Overloaded heavy vehicles (HVs) have significant negative impacts on traffic conditions due to their inferior driving performance. Highway authorities need to understand the impact of overloaded HVs to assess traffic conditions and set management strategies. We propose a multi-class traffic flow model based on Smulders fundamental diagram to analyze the influence of overloaded HVs on traffic conditions. The relationship between the overloading ratio and maximum speed is established by freeway toll collection data for different types of HVs. Dynamic passenger car equivalent factors are introduced to represent the various impacts of overloaded HVs in different traffic flow patterns. The model is solved analytically and discussed in detail in the appendices. The model validation results show that the proposed model can represent traffic conditions more accurately with consideration for overloaded HVs. The scenario tests indicate that the increase of overloaded HVs leads to both a higher congestion level and longer duration.

Keywords: freeway traffic operation and management; multi-class traffic flow model; analytical method; overloaded HVs

1. Introduction

Heavy vehicles (HVs) have significant impacts on traffic conditions. However, it is a common practice in China for commercial carriers to overload (i.e., load trucks with goods heavier than the factory recommended weight limit) their fleets to reduce their operating costs [1]. Compared with conforming HVs, overloaded ones suffer from lower speeds, inferior acceleration and deceleration performances, and, consequently, impose more significant impacts on traffic conditions.

Unfortunately, overloaded HVs are frequently observed on freeways in most parts of China and many developing countries, such as India, Thailand, Vietnam, etc. In China, if one heavy vehicle is detected as an overloaded heavy vehicle, the toll station staffs will still allow this heavy vehicle entering the freeway but charge additional fines for overloading. This is because there is not enough space to unload and temporarily store the overloaded goods in the toll station plaza, and the long stop at the toll station will obstruct the subsequent vehicles entering the freeway. Therefore, the toll station staff will not forbid the overloaded HVs entering the freeway, but punish with fines, which mainly considers the pavement fatigue, but not the negative impacts on traffic condition. However, the profit from overloading can cover the additional cost and, therefore, many heavy vehicles choose to overload. For example, the average overloading proportion (i.e., the total number of overloaded HVs/population of HVs) on the freeway is 15%, and it could be more than 40% at midnight in eastern China. Furthermore, the average overloading ratio (i.e., (total weight – weight limit)/weight limit) is 35%, and the overloading ratio of tractor-trailers could exceed 100% in some extreme circumstances [2,3].

The average reduction of overloaded HVs' travel speeds is 16% compared with HVs with the same configuration but loaded at capacity [4].

The problems induced by overloaded HVs are significant, and there are a number of studies that focus on the impacts on pavement fatigue life and distress, while the impacts of overloaded HVs on freeway traffic conditions have not been properly analyzed to the best of our knowledge. The effect of HVs is captured by the Passenger Car Equivalent (PCE) factor in the Highway Capacity Manual (HCM 2010) [5]. However, the different effects of overloaded and normal HVs are not distinguished. Moreover, the impacts of HVs vary from different traffic conditions [6], while the fixed PCE factors in the HCM are sensitive neither to the presence of overloaded HVs nor to various traffic conditions. This research aims to quantitatively evaluate the traffic impact of overloaded HVs on traffic conditions, and this will contribute to refine the management strategies of freeway overloaded HVs and guarantee the sustainable development of freeway transportation.

We developed a multi-class traffic flow model to analyze the impact of overloaded HVs on traffic conditions. The model can be used to estimate traffic conditions in real-time and evaluate traffic management strategies with consideration for the presence of overloaded HVs. First, the relationship between vehicle weight and driving performance is established to distinguish the diverse driving performances between overloaded HVs and normal ones. Next, a dynamic PCE is introduced to represent the diverse impacts of overloaded HVs under different traffic conditions. Then, the formulation of effective density and effective volume is proposed. After that, an empirical study is conducted to evaluate the accuracy of the proposed model. Finally, several scenario tests are performed to verify the model results and to represent the sensitivity of overloaded HVs with different overloading proportions.

The paper is organized as follows: Section 2 summarizes the previous research in multi-class traffic flow models and the development of dynamic PCE. Section 3 describes the freeway toll data used in this study and the relationship between the overloading ratio and maximum speed. Section 4 discusses the process to establish the multi-class kinematic wave traffic flow model. Section 5 presents an empirical study to validate model results with real traffic data. Section 6 presents several scenario tests to show the impacts of overloaded HVs in different traffic demand and supply combinations. Finally, Section 7 concludes the study with a discussion of the study results and suggestions for future research.

2. Literature Review

Overloaded HVs, characterized by their inferior driving performance (such as lower running speed and larger minimum safe headway), tend to impose negative impacts on traffic conditions under different traffic flow patterns. However, the impact of overloaded HVs has not been carefully addressed in previous multi-class macroscopic traffic flow models.

The presence of HVs causes larger space and time headways and longer reaction time [7]. Vehicle weight is one of the critical factors that determine running, braking, and handling performance [8]. For example, the minimum safe headway of HVs depends on reaction time and stopping distances, which, in turn, depend on the total vehicle weight. Therefore, overloaded HVs need larger headways than normal ones. Meanwhile, the desired travel speed is not only limited by traffic conditions but also constrained by the vehicle's own weight [9]. The desired travel speed decreases with increased vehicle weight in the free flow condition. Thus, overloaded HVs need to be considered separately when analyzing their impacts on traffic conditions due to distinguishable driving performance.

PCE describes the relative impact of a vehicle on traffic conditions when compared with a typical passenger car. In the development of PCE, the equivalency criterion varies from flow rates and density, headways, queue discharge flow, speed, delays, v/c ratio, etc. [10,11]. The PCE value of each vehicle type is typically constant. However, the impact of HVs varies under different traffic conditions [12]. It is noticed that the impact of HVs under congestion is greater than under the free-flow condition [13].

The cycle of acceleration-deceleration is more recurrent under congestion since the acceleration and deceleration performances of HVs are inferior. Moreover, it is also mentioned that PCE depends on the presence of HVs [5,14]. When there are more HVs on a freeway, the HVs could form platoons and have less interaction with passenger cars. Thus, the PCE of each HV in platoons should be smaller than individual HVs, although the total impacts from HVs increase with the amount of HVs. In conclusion, the previous studies suggest that the PCE of HVs should vary with traffic conditions and the proportion of HVs. Mehar (2013) [15] suggested PCU values for different types of vehicles at different levels of service and for different traffic compositions. Van Lint (2008) [16] proposed a continuous dynamic PCE based on space occupancy. The dynamic PCE value depends on speed, time headway, and vehicle length of both HVs and passenger cars. However, the dynamic PCE is not sensitive to the proportion of HVs, and the more severe impact of overloaded HVs on traffic conditions is not considered in this PCE formulation.

Recently, multi-class traffic flow models have been discussed frequently in order to describe non-linear traffic phenomena, which cannot be reproduced by aggregate class models [17,18]. In order to identify driving characteristics among different vehicle types and simultaneously reduce computational burdens for online traffic control, multi-class kinematic wave traffic flow models are proposed [19,20]. In multi-class kinematic wave traffic flow models, vehicle types are distinguished by driving performance and vehicle physical properties, such as speed and vehicle length. Daganzo (2002) [21] proposed a multi-class model for two vehicle types (i.e., passenger car and HV) according to travel speed. Chanut and Buisson (2003) [22] pointed out that vehicles are differentiated not only by their speeds but also by their lengths, and they established a two-flow traffic model. Ngoduy and Liu (2007) [23] formulated a multi-class first-order traffic flow model for the faster car, slower car, and HV vehicle types, where each type is characterized by their desired speeds in free-flow and all vehicles are traveling at the same speed under congestion. Van Wageningen-Kessels (2013, 2014) [24,25] developed a multi-class continuum traffic flow model that accounts for the differences between vehicle types, such as maximum speed, headway, and vehicle length.

Although travel speed has been consistently identified as a critical factor for vehicle type identification, overloaded HVs have never been classified as a standalone vehicle type in previous literature. The contributions of this study include the following.

- (1) A new dynamic PCE was designed for overloaded HVs, and it can represent the different influences present when traffic conditions change.
- (2) A new multi-class kinematic wave traffic flow model based on dynamic PCE is proposed with consideration for the driving performances of overloaded HVs.
- (3) The impacts of overloaded HVs on freeway traffic conditions are analyzed based on scenario tests.

3. Data and Vehicle Type Description

3.1. Freeway Toll Data

Each vehicle enters and exits the freeway by toll station in China, and the freeway toll data contains the trip information of each vehicle traveling on a freeway, such as the entry/exit time, entry/exit station, total weight, and vehicle type (i.e., the weight-limit can be known for each heavy vehicle). The toll fee for heavy vehicles is based on the vehicle type, travel distance, and total weight. In this case, each entrance ramp of toll station is equipped with a wagon balance to obtain the weight information of each vehicle. Therefore, it is easy to confirm whether one heavy vehicle is overloaded or not, and the overloading proportion and ratio can be calculated accurately by the freeway toll data. The traffic conditions, including traffic demand and travel time, can be estimated using freeway toll data with proper data quality control [26]. The real travel time, which will be used to acquire free-flow travel speeds for model calibration and validation in each time interval, can be calculated using Equation (1):

$$T_{(i,j)}^k = \frac{\sum_{n=1}^{N_{(i,j)}^k} (t_{en(n)}^k - t_{ex(n)}^k)}{n_{(i,j)}^k} - (t_{on(i)}^k + t_{off(j)}^k) \quad (1)$$

where $T_{(i,j)}^k$ is the travel time from entry station i to exit station j during time period k , $N_{(i,j)}^k$ is the sample size from toll station i to j after data quality control during time period k , $t_{en(n)}^k$ is the entry time of vehicle n entering during time period k , $t_{ex(n)}^k$ is the exit time of vehicle n , and $t_{on(i)}^k$ and $t_{off(j)}^k$ are the travel time on the on-ramp of entry station i and the off-ramp of exit station j , respectively, which can be calculated using the loop detector data on the ramp.

3.2. Characteristics of Different Vehicle Types

Freeway toll data records the vehicle type of passenger cars (i.e., PC1, PC2, . . . , PC4) and heavy vehicles (i.e., HV1, HV2, . . . , HV5) separately. PCs are classified by vehicle capacity while HVs are classified by total weight limit. Based on the vehicle type information, the volume proportion of PC1 can be calculated. Additionally, the travel speed of each vehicle can be calculated by entry/exit time and the distance between the entry/exit stations. The freeway toll data of the whole Jiangsu freeway network during July 2012 were utilized, and the characteristics of each classification are shown in Table 1. In most cases, small passenger cars (i.e., PC1, the type 1 passenger car) comprise the largest proportion of traffic volume on the freeway. For example, the freeway volume proportion of PC1 in Jiangsu province is 68.6% (Table 1), while the subtotal of PC2 (i.e., the type 2 passenger car), PC3, and PC4 altogether is merely 4.3%. Since PC2, PC3, and PC4 only comprise a small proportion of the vehicle population, these volumes are omitted in the modeling process for simplification. In this study, only PC1, HV1 (i.e., the type 1 heavy vehicle), HV2, HV3, HV4, and HV5 are modeled.

Table 1. Characteristics of different passenger cars and heavy vehicles.

| Type ID | Classification Criteria PC: Vehicle Capacity HV: Total Weight Limit | Vehicle Length (m) | Traffic Volume Proportion in Jiangsu Province (%) | 90% Percentile Highest Travel Speed (km/h) |
|---------|---|--------------------|---|--|
| PC1 | ≤7 seats | 3.5–6 | 68.6 | 117.5 |
| PC2 | 8–9 seats | 6–9 | 2.0 | 100.9 |
| PC3 | 20–29 seats | 9–12 | 0.9 | 95.4 |
| PC4 | ≥40 seats | 12–13.7 | 1.3 | 93.8 |
| HV1 | ≤2 t | 3.5–4.5 | 6.2 | 90.6 |
| HV2 | 2–5 t (inclusive of 5 t) | 4.5–6 | 9.1 | 87.2 |
| HV3 | 5–10 t (inclusive of 10 t) | 6–8 | 4.1 | 84.1 |
| HV4 | 10–15 t (inclusive of 15 t) | 8–12 | 4.5 | 82.0 |
| HV5 | >15 t | 12–16.5 | 3.3 | 79.0 |

Due to their different mechanical performances, each vehicle type has a specific maximum speed in the free flow condition. Taking the 90th percentile of the highest travel speed as the maximum speed of each vehicle type (non-overloaded vehicles) in free-flow, the results are shown in Table 1. The largest speed gap existing between PC1 and HV5 is 38.5 km/h.

3.3. Overloading Ratio and Maximum Speed

Maximum speed is a significant parameter of traffic flow models, and the maximum speed of heavy vehicles is directly impacted by overloading ratio (i.e., (total weight – weight limit)/weight limit). To analyze the relationship between overloading ratio and maximum speed, the toll station data of HVs with entering and exiting times both between 0:00 and 6:00 a.m. were selected to approximate the free-flow condition. According to the collected data, the maximum speeds decrease with increased vehicle size (as seen in Figure 1a), and the overloaded HVs are slower than the normal ones. The overloading ratio of each HV was aggregated by an increment of 1%. Then, the 90th

percentile of the speed in each increment interval was assumed to be the maximum speed for a specific overloading ratio. Lastly, the maximum speeds were regressed by ordinary least squares (i.e., OLS) against the aggregated overloading ratio for each HV type (as seen in Figure 1b–f).

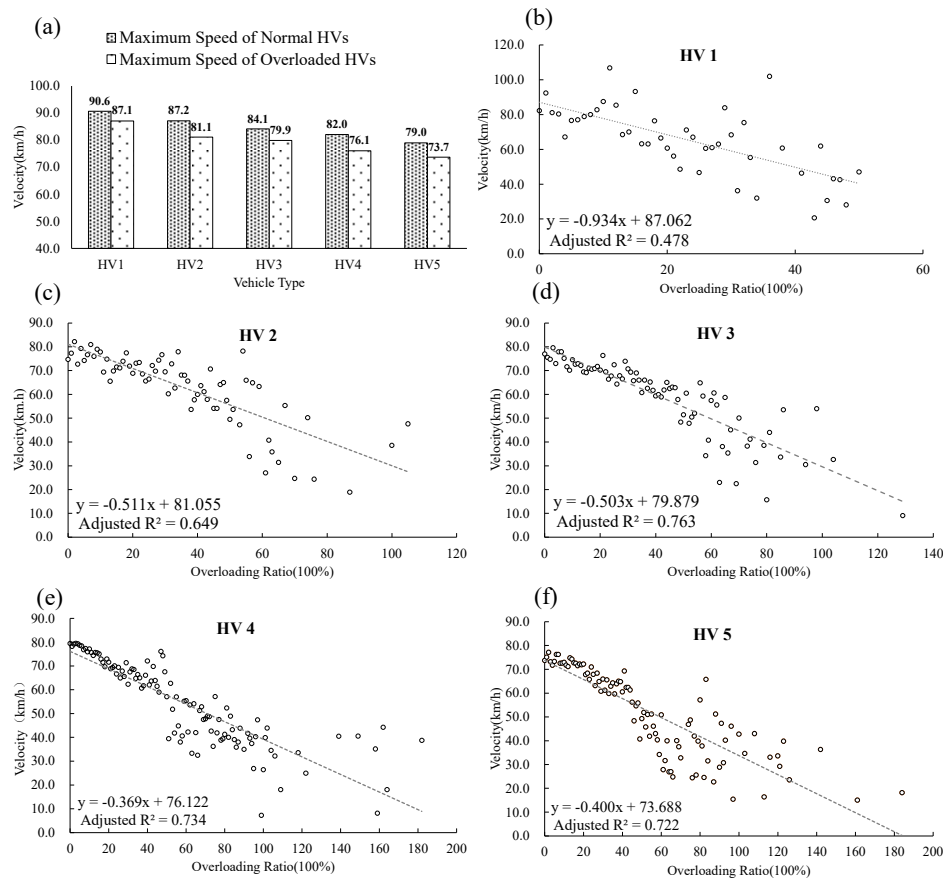


Figure 1. (a) Difference of the maximum speed between overloaded HVs and normal HVs. (b–f) Relationship between the maximum speeds and overloading ratio among different types of HVs.

It is obvious that the maximum speed decreases with the increased overloading ratio in each HV type. The statistic results of each regression model are shown in Table 2. Significance F and P -value of all the five regression models are below than 0.05. The results indicate that the overloading ratio has a significant negative impact on the maximum speed in each HV type. HV1 has a lower adjusted R^2 value that is smaller than 0.5. The main reason is that there are few overloaded HV1 on the freeway and the overloading ratio is not as large as the other HV types (e.g., the maximum overloading ratio of HV1 is 0.5). It can also be noticed that the fitness is inferior when the overloading ratio is high. The main reason is that there are few samples with high overloading ratio, hence, the 90th percentile of the highest speed could be dispersed. Another potential reason is that the driving behavior of the high overloaded HVs varies greatly. Some drivers realize the danger of overloading and choose to drive at a low speed, while some drive as fast as they can.

The regression results (Table 2) can be used to calculate the maximum speeds of different HV types as the input of the proposed model with considerations for overloaded HVs. The OLS regression model can be represented in its reduced form as:

$$v_{u,\max}^r = g_u(r) = C_u - \beta_u \cdot r \quad (2)$$

where $v_{u,\max}^r$ is the maximum speed of vehicle type u when the overloading ratio is r . C_u and β_u are the constant and coefficient of vehicle type u , respectively.

Table 2. Statistical characteristics of regression coefficients for different HVs.

| Vehicle Type | Coefficients | t Stat | P-Value | Lower 95% | Upper 95% | Adjusted R ² | F-Statistic | Significance F | Observations | | | | | | | | | | | | | | | | | | | | | | | | | | | | | | | | | | | | | | | | | | | | | | | | | | | | | | | | | | | | | | | | |
|--------------|--------------|--------|---------|-------------------------|-----------|-------------------------|-------------|----------------|-------------------------|-----|-----|----------|--------|--------|-------------------------|--------|--------|-------|---------|-------------------------|-----|-----------|--------|---------|-------------------------|--------|--------|-----|----------|--------|--------|-------------------------|--------|--------|-------|---------|-------------------------|-----|-----------|--------|---------|-------------------------|--------|--------|-----|----------|--------|--------|-------------------------|--------|--------|-------|---------|-------------------------|-----|-----------|--------|---------|-------------------------|--------|--------|-----|----------|--------|--------|-------------------------|--------|--------|-------|---------|-------------------------|-----|-----------|
| HV1 | Constant | 87.062 | 21.592 | 1.053×10^{-24} | 78.930 | 95.194 | 0.478 | 39.440 | 1.430×10^{-07} | 45 | | | | | | | | | | | | | | | | | | | | | | | | | | | | | | | | | | | | | | | | | | | | | | | | | | | | | | | | | | | | | | | |
| | β_u | -0.934 | -6.280 | 1.430×10^{-07} | -1.235 | -0.634 | | | | | HV2 | Constant | 81.055 | 40.852 | 4.419×10^{-49} | 77.095 | 85.016 | 0.649 | 123.983 | 6.885×10^{-17} | 69 | β_u | -0.511 | -11.135 | 6.885×10^{-17} | -0.602 | -0.419 | HV3 | Constant | 79.879 | 50.288 | 9.353×10^{-62} | 76.717 | 83.040 | 0.763 | 254.289 | 2.059×10^{-26} | 81 | β_u | -0.503 | -15.946 | 2.059×10^{-26} | -0.566 | -0.440 | HV4 | Constant | 76.122 | 50.173 | 1.239×10^{-77} | 73.115 | 79.129 | 0.734 | 303.644 | 2.033×10^{-33} | 112 | β_u | -0.369 | -17.425 | 2.033×10^{-33} | -0.411 | -0.327 | HV5 | Constant | 73.688 | 44.483 | 2.998×10^{-67} | 70.401 | 76.975 | 0.722 | 257.511 | 2.681×10^{-29} | 101 | β_u |
| HV2 | Constant | 81.055 | 40.852 | 4.419×10^{-49} | 77.095 | 85.016 | 0.649 | 123.983 | 6.885×10^{-17} | 69 | | | | | | | | | | | | | | | | | | | | | | | | | | | | | | | | | | | | | | | | | | | | | | | | | | | | | | | | | | | | | | | |
| | β_u | -0.511 | -11.135 | 6.885×10^{-17} | -0.602 | -0.419 | | | | | HV3 | Constant | 79.879 | 50.288 | 9.353×10^{-62} | 76.717 | 83.040 | 0.763 | 254.289 | 2.059×10^{-26} | 81 | β_u | -0.503 | -15.946 | 2.059×10^{-26} | -0.566 | -0.440 | HV4 | Constant | 76.122 | 50.173 | 1.239×10^{-77} | 73.115 | 79.129 | 0.734 | 303.644 | 2.033×10^{-33} | 112 | β_u | -0.369 | -17.425 | 2.033×10^{-33} | -0.411 | -0.327 | HV5 | Constant | 73.688 | 44.483 | 2.998×10^{-67} | 70.401 | 76.975 | 0.722 | 257.511 | 2.681×10^{-29} | 101 | β_u | -0.400 | -16.047 | 2.681×10^{-29} | -0.449 | -0.350 | | | | | | | | | | | | |
| HV3 | Constant | 79.879 | 50.288 | 9.353×10^{-62} | 76.717 | 83.040 | 0.763 | 254.289 | 2.059×10^{-26} | 81 | | | | | | | | | | | | | | | | | | | | | | | | | | | | | | | | | | | | | | | | | | | | | | | | | | | | | | | | | | | | | | | |
| | β_u | -0.503 | -15.946 | 2.059×10^{-26} | -0.566 | -0.440 | | | | | HV4 | Constant | 76.122 | 50.173 | 1.239×10^{-77} | 73.115 | 79.129 | 0.734 | 303.644 | 2.033×10^{-33} | 112 | β_u | -0.369 | -17.425 | 2.033×10^{-33} | -0.411 | -0.327 | HV5 | Constant | 73.688 | 44.483 | 2.998×10^{-67} | 70.401 | 76.975 | 0.722 | 257.511 | 2.681×10^{-29} | 101 | β_u | -0.400 | -16.047 | 2.681×10^{-29} | -0.449 | -0.350 | | | | | | | | | | | | | | | | | | | | | | | | | | | | | |
| HV4 | Constant | 76.122 | 50.173 | 1.239×10^{-77} | 73.115 | 79.129 | 0.734 | 303.644 | 2.033×10^{-33} | 112 | | | | | | | | | | | | | | | | | | | | | | | | | | | | | | | | | | | | | | | | | | | | | | | | | | | | | | | | | | | | | | | |
| | β_u | -0.369 | -17.425 | 2.033×10^{-33} | -0.411 | -0.327 | | | | | HV5 | Constant | 73.688 | 44.483 | 2.998×10^{-67} | 70.401 | 76.975 | 0.722 | 257.511 | 2.681×10^{-29} | 101 | β_u | -0.400 | -16.047 | 2.681×10^{-29} | -0.449 | -0.350 | | | | | | | | | | | | | | | | | | | | | | | | | | | | | | | | | | | | | | | | | | | | | | |
| HV5 | Constant | 73.688 | 44.483 | 2.998×10^{-67} | 70.401 | 76.975 | 0.722 | 257.511 | 2.681×10^{-29} | 101 | | | | | | | | | | | | | | | | | | | | | | | | | | | | | | | | | | | | | | | | | | | | | | | | | | | | | | | | | | | | | | | |
| | β_u | -0.400 | -16.047 | 2.681×10^{-29} | -0.449 | -0.350 | | | | | | | | | | | | | | | | | | | | | | | | | | | | | | | | | | | | | | | | | | | | | | | | | | | | | | | | | | | | | | | | | | | |

It can be found that the constants and β_u vary from different HV types in Table 2. The constants represent the maximum speeds of each HV type under different overloading ratio, and the regression slopes represent the reduction rate of maximum speeds. The results indicate that HV1 has the highest maximum speed and HV5 has the lowest one when comparing with the other HV types. It is explicable because HV1 and HV5 have the smallest and largest vehicle size and weight capacity, respectively, as seen in Table 1. Meanwhile, the regression slopes (i.e., coefficients) show that HV1 has the highest reduction rate, and the slope appears downtrend when HV has a larger size (i.e., HV2, HV3, HV4, HV5). This is also reasonable because small HVs always have the lower maximum engine power than large HVs, and the maximum speeds of small HVs are more sensitive with the overloading ratio.

4. Multi-Class Traffic Flow Model with Overloaded HVs

4.1. Multi-Class Fundamental Diagram

In continuous traffic flow, fundamental diagrams are used to describe the relationship of traffic state variables, including speed, density, and volume. Several principles (or assumptions) form the foundation of multi-class continuum traffic flow models to guarantee the existence and uniqueness of the model solution, and several requirements are needed to verify whether the proposed model has qualitatively desirable properties. The principles and requirements are outlined in Table 3 [20,25].

Table 3. Principles and requirements of multi-class traffic flow models.

| Principles | Requirements |
|---|--|
| P1. Multi-class traffic flow is a continuous flow. | R1. Given the density of each vehicle type, the class-specific speeds and flows are defined uniquely. |
| P2. Vehicles are conserved between adjacent segments, and they can only enter or exit through the freeway toll station. | R2. The model has a unique solution on the maximum flow (i.e., capacity). |
| P3. Traffic flow is a single-pipe flow, and the lane number only affects the segment capacity. | R3. In free flow, the speeds of each vehicle type can be different and are allowed to be constant or decrease with increasing density. |
| P4. Traffic flow is always in two regimes: free flow or congestion. | R4. In congestion, the speeds of each vehicle type have to decrease monotonously with density, and the speeds should be equal due to car-following driving behavior. |
| P5. Traffic is always in the equilibrium state. | R5. If the density reaches a certain threshold, the speeds of each vehicle type are all zero. |
| P6. Traffic consists of homogeneous groups of vehicles and drivers. | R6. If the density is zero, the speeds of each vehicle type are the class-specific free flow speed. |

The shape of the fundamental diagram is based on principles and requirements. First, the fundamental diagram should be able to differentiate each vehicle type. Additionally, all the vehicle types should be in the free flow or congestion regime at the same time. Furthermore, in free flow, the speeds of each type can differ. In congestion, they should be equal. Daganzo and Greenshields fundamental diagram cannot satisfy the above principles and requirements. For the Daganzo diagram, the speeds of each vehicle type can differ in free-flow, while it is difficult to guarantee all the vehicle types are in the same traffic condition regime. For the Greenshields diagram, the requirements of the speeds in free-flow and congestion cannot both be guaranteed.

The Smulders fundamental diagram [27] is a combination of the Greenshields fundamental diagram [28] and the Daganzo fundamental diagram [29]. In free-flow, the density-speed panel of the Smulders diagram is identical to the Greenshields diagram, i.e., the speed decreases with increasing density, which is more suitable for empirical data [30]. While in congestion, the density-volume panel of the Smulders diagram is identical to that of the Daganzo diagram, in which the relationship between

density and volume is linear. In this study, the Smulders fundamental diagram is chosen as the basis of the freeway multi-class traffic flow model, and the multi-class Smulders fundamental diagram [23] is shown in Figure 2.

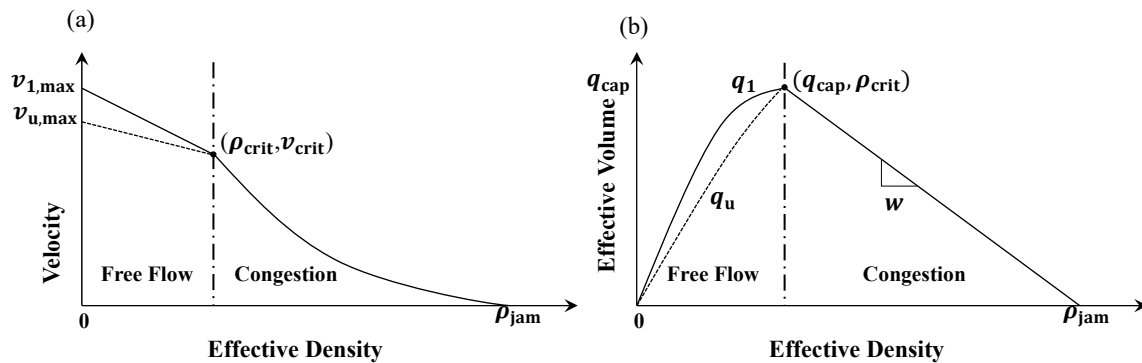


Figure 2. Multi-class traffic flow fundamental diagram. (a) Density–speed panel. (b) Density–volume panel.

Effective density and effective volume are used to represent the average traffic conditions of multi-class traffic flow on one link. The calculation of effective density and effective volume will be discussed in Section 4.4. The multi-class fundamental diagram of the density-speed panel is represented by the following equations.

Free flow ($0 \leq \rho_e < \rho_{crit}$):

$$v_u = v_{u,max} - \frac{v_{u,max} - v_{crit}}{\rho_{crit}} \rho_e \tag{3}$$

Congestion ($\rho_{crit} \leq \rho_e < \rho_{jam}$):

$$v_u = w \left(\frac{\rho_{jam}}{\rho_e} - 1 \right) \tag{4}$$

$$w = \frac{\rho_{crit} v_{crit}}{\rho_{jam} - \rho_{crit}} \tag{5}$$

where ρ_e is the effective density, ρ_{crit} is the critical density, ρ_{jam} is the jam density, subscript u is the vehicle type, v_u is the speed of vehicle type u , $v_{u,max}$ is the maximum speed of vehicle type u , v_{crit} is the critical speed, and w is the shockwave speed.

4.2. Definition of Dynamic PCE

The impact of one vehicle on the traffic condition depends on its space occupancy, i.e., the vehicle length plus the space between the two adjacent vehicles [16,24], which is a dynamic variable that changes with speed and headway based on the safe-distance model [31]. This means one vehicle has more influences on traffic condition when it occupies more road space. Moreover, it has been learned that the PCE of HV decreases when the number of HVs increases because the impact of one HV in a platoon is less severe than one in a stream [5,32]. Based on the above discussions, the dynamic PCE of HV class u is defined as a combination of relative space occupancy (i.e., the ratio of space occupancy between class u and passenger car unit) and its proportion to the passenger car:

$$\eta_{u,i} = f(p_{u,i}) \cdot \frac{v_{u,i} \cdot T_{u,i} + L_u}{v_{1,i} \cdot T_{1,i} + L_i} \tag{6}$$

$$f(p_{u,i}) = \frac{1}{1 + \alpha \cdot p_{u,i}} \tag{7}$$

$$p_{u,i} = \frac{N_{u,i}}{N_{1,i} + N_{u,i}} \tag{8}$$

where the passenger car is represented by $u = 1$, $\eta_{u,i}$ is the dynamic PCE of vehicle type u on link i , $T_{u,i}$ is the headway of vehicle type u on link i (which will be discussed in Section 4.3), L_u is the length of vehicle type u , and $p_{u,i}$ is the proportion of vehicle type u against the total number of the passenger car and vehicle type u (not the total vehicles) on link i . $N_{u,i}$ and $N_{1,i}$ are the number of vehicle type u and passenger cars on link i , respectively. α is the adjustment ratio of the HV proportion, and it was utilized to represent how the influence degree of each HV reduces when the proportion of HVs increases. The appropriate range of the adjusted factor should ensure $f(p_{u,i}) \in (0, 1]$, so that $\alpha \geq 0$.

4.3. Relationship between Vehicle Weight and Minimum Safe Headway

4.3.1. Free-Flow

It is assumed that the brake system of one vehicle type provides the same brake power. The stopping distance of normal and overloaded HVs in free flow, based on the kinetic energy theorem, is represented as follows:

$$S_u = \frac{m_u v_u^2}{2F_u}; S_u^r = \frac{m_u^r (v_u^r)^2}{2F_u} \quad (9)$$

where u is the vehicle type of HV. S_u and S_u^r are the stopping distance of normal and overloaded HVs, respectively. m_u and m_u^r is the total weight of normal and overloaded HVs. v_u and v_u^r are the travel speed of normal and overloaded HVs, respectively. F_u is the maximum brake force. To avoid a rear-end collision, the minimum safe headway between the rear of the leading vehicle and the head of the following vehicle is represented as:

$$T_u = \frac{S_u}{v_u} = \frac{m_u v_u}{2F_u}; T_u^r = \frac{S_u^r}{v_u^r} = \frac{m_u^r v_u^r}{2F_u} \quad (10)$$

$$T_u^r = \frac{m_u^r v_u^r}{m_u v_u} T_u \quad (11)$$

where T_u and T_u^r are the minimum safe headways of normal and overloaded HVs, respectively. According to Equations (2), (3), (11), and set $\frac{m_u^r}{m_u} = r + 1$, T_u^r can be written as:

$$T_u^r = (r + 1) \cdot \frac{g_u(r)\rho_{\text{crit}} - [g_u(r) - v_{\text{crit}}]\rho_e}{v_{u,\text{max}}\rho_{\text{crit}} - (v_{u,\text{max}} - v_{\text{crit}})\rho_e} \cdot T_u \quad (12)$$

4.3.2. Congestion

All the vehicles are assumed to have the same speed in congestion. According to Equation (11), the relationship between the minimum safe headways of normal HVs and overloaded HVs is calculated as follows:

$$T_u^r = \frac{m_u^r}{m_u} T_u = (r + 1) T_u \quad (13)$$

4.4. Effective Density and Effective Volume

4.4.1. Effective Density

The effective density of multi-class traffic flow is defined as a weighted sum of the density of each vehicle type:

$$\rho_{e(i)}^k = \sum_u \eta_{u,i}^k \rho_{u,i}^k \quad (14)$$

where $\eta_{u,i}^k$ is the dynamic PCE of vehicle type u on link i at time interval k , and $\rho_{u,i}^k$ is the density of vehicle type u on link i at time interval k . The calculation of $\rho_{u,i}^k$ in this study can be found in Appendix B. The subscripts i and k are omitted for the remainder of this chapter for simplicity.

To use one formula to represent the effective density in both free-flow and in congestion using only known variables, necessary transformations of effective density have been done in Appendix A.1. The boundary conditions on the parameters (i.e., maximum speed and minimum safe headway) are discussed to ensure the existence of a solution to a quadratic equation about effective density and to choose the right root. The detail process can be found in Appendix A. To summarize, the formulation of effective density is:

$$\rho_e = \frac{(-a_1 + \sum_u f(p_u)\rho_u b_u) + \sqrt{(a_1 - \sum_u f(p_u)\rho_u b_u)^2 + 4b_1 \sum_u f(p_u)\rho_u a_u}}{2b_1} \quad (15)$$

where $f(p_u) = \frac{1}{1+\alpha \cdot p_u}$.

In free flow, it is $a_u^f = L_u + T_u v_{u,\max}$, $b_u^f = -T_u \frac{v_{u,\max} - v_{\text{crit}}}{\rho_{\text{crit}}}$.

In congestion, it is $a_u^c = T_u w \rho_{\text{jam}}$, $b_u^c = L_u - T_u w$; $w = \frac{\rho_{\text{crit}} v_{\text{crit}}}{\rho_{\text{jam}} - \rho_{\text{crit}}}$.

When there are overloaded HVs, it is $v_{u,\max}^r = g_u(r)$.

In free flow, it is $T_u^r = (r+1) \cdot \frac{g_u(r)\rho_{\text{crit}} - [g_u(r) - v_{\text{crit}}]\rho_e}{v_{u,\max}\rho_{\text{crit}} - (v_{u,\max} - v_{\text{crit}})\rho_e} \cdot T_u$.

In congestion, it is $T_u^r = (r+1)T_u$.

4.4.2. Effective Volume of Multi-Class Traffic Flow

After getting the effective density, the speed of vehicle type u (i.e., v_u) can be calculated using Equations (3) or (4). Then, the dynamic PCE (i.e., η_u) also can be obtained. At last, the effective volume of vehicle type u (i.e., $q_{e(u)}$), can be calculated using the following equation:

$$q_{e(u)} = \eta_u \cdot \rho_u \cdot v_u \quad (16)$$

The total effective volume on link i is the sum of all types of vehicles:

$$q_e = \sum_u q_{e(u)} \quad (17)$$

5. Validation of Model Results

5.1. Model Preparation

A segment of G15 freeway in Jiangsu Province, China was selected to evaluate the model performance empirically. The segment connects a mainline toll station named Sulu station and its adjacent ramp toll station named Haitou station. The analyzed travel direction is from the mainline toll station to the ramp toll station. The total travel distance is 28 km, and there are two lanes in the travel direction. In addition, there is no other on/off ramp or service area between these two toll stations, so all the vehicles that entered the selected segment can be captured by toll station data from the mainline.

All of the parameters are shown in Table 4. The parameters of each vehicle type are based on the results of Table 1, and the parameters of the freeway segment are obtained from HCM 2010 [5] and the Jiangsu Freeway Traffic Condition Analyzing Report [4].

Table 4. Parameters of the model.

| Parameters | Unit | Definition | PC1 | HV1 | HV2 | HV3 | HV4 | HV5 |
|---------------|----------|--|-------|------|------|-------|------|------|
| L_u | m | the vehicle length of type u | 5 | 4 | 5 | 7 | 12 | 13 |
| $v_{u,max}$ | km/h | the maximum speed of type u | 117.5 | 90.6 | 87.2 | 84.1 | 82.0 | 79.0 |
| $v_{u,max}^w$ | km/h | the maximum speed of overloaded type u | | 87.1 | 81.1 | 79.9 | 76.1 | 73.7 |
| T_u | s | the minimum safe headway of type u | 1 | 1 | 1.5 | 2 | 2.5 | 2.5 |
| q_{crit} | pce/h/ln | the capacity of single lane | | | | 2200 | | |
| v_{crit} | km/h | the critical speed | | | | 60 | | |
| ρ_{crit} | pce/m/ln | the critical density | | | | 0.037 | | |
| ρ_{jam} | pce/m/ln | the jam density | | | | 0.2 | | |
| α | unit | adjustment ratio of proportion | | | | 0.93 | | |

5.2. Model Results versus Real Traffic Data

The freeway segment suffers from high heavy vehicle volumes on Monday and Friday each week, and the peak hour ranges from 9:00 a.m. to 14:00 p.m. In order to evaluate the proposed model performance both in weekday and weekend, the real traffic data from July 1st (Sunday), 2nd (Monday), 4th (Wednesday), and 27th (Friday) of 2012 were chosen for model validation. The analyzing time period was from 8:00 a.m. to 15:00 p.m., which covers the AM peak and PM peak of the selected segment. The time interval was 15 min, which is widely used in traffic management and time-dependent traffic condition analysis. Because the initial network is empty, the demand loading time should be prior to the analyzing time period, otherwise, the model will cause the prediction of an unrealistically higher travel speed. In this practical application, the demand loading started at 6:30 a.m., and then the extract the time period of 8:00 a.m.–15:00 p.m. took place to evaluate the model performance.

In the first model run, overloaded HVs were treated as normal HVs. In the second model run, overloaded HVs and the normal ones were separated. The overloading ratio of each HV may be different. In order to obtain the overloading ratio r in Equation (2) for each time interval, the overloading ratio was averaged within each time interval by freeway toll data, and then the maximum speed of overloaded HVs was calculated using the regression model in Equation (2). The field data was calculated using Equation (1), and the travel times of PC1 were converted into speed for comparison in Figure 3.

As seen in Figure 3, the proposed model can represent the time-dependent speed variation of PC1 when compared with the field data, and the difference between the results when considering the overloaded HVs or not can be observed.

Analysis of variance (ANOVA) is implemented to check whether considering the overloaded HVs makes differences on the traffic condition of the freeway segment. Set $\alpha = 0.05$, and the results are shown in Table 5.

It can be found that the F -values of the four test days are all larger than F_{crit} , and P -values are all below 0.05. The results indicate that there are significant differences on traffic condition when considering the overloaded HVs or not.

Based on the proposed multi-class traffic flow model in Section 4, the free flow speed and minimum safe distance are affected by the overloading ratio. Then, the dynamic PCE changes based on the space occupancy of the overloaded HVs. Finally, the effective density is affected, and the travel speed of each vehicle type changes based on the calibrated multi-class traffic flow diagram. When considering the overloaded HVs, the effective density will be a bit higher and the travel speed will be lower. It is noticeable that speed values are different between the overloaded HVs and non-overloaded HVs model, but not the changing trend. Since these two models are both based on the Smulders fundamental diagram, the speed curves with/without consideration for overloaded HVs will be similar unless there is an extremely high proportion of overloaded HVs with high overloading ratio.

Table 5. Analysis of variance about the model results considering overloaded HVs or not.

| Test Date | Mean Square Error | F | P-Value | F _{crit} |
|-----------|-------------------|--------|---------|-------------------|
| 1 July | 26.841 | 10.370 | 0.002 | 4.020 |
| 2 July | 45.108 | 6.096 | 0.017 | 4.020 |
| 4 July | 43.507 | 11.180 | 0.002 | 4.020 |
| 27 July | 37.815 | 7.874 | 0.007 | 4.020 |

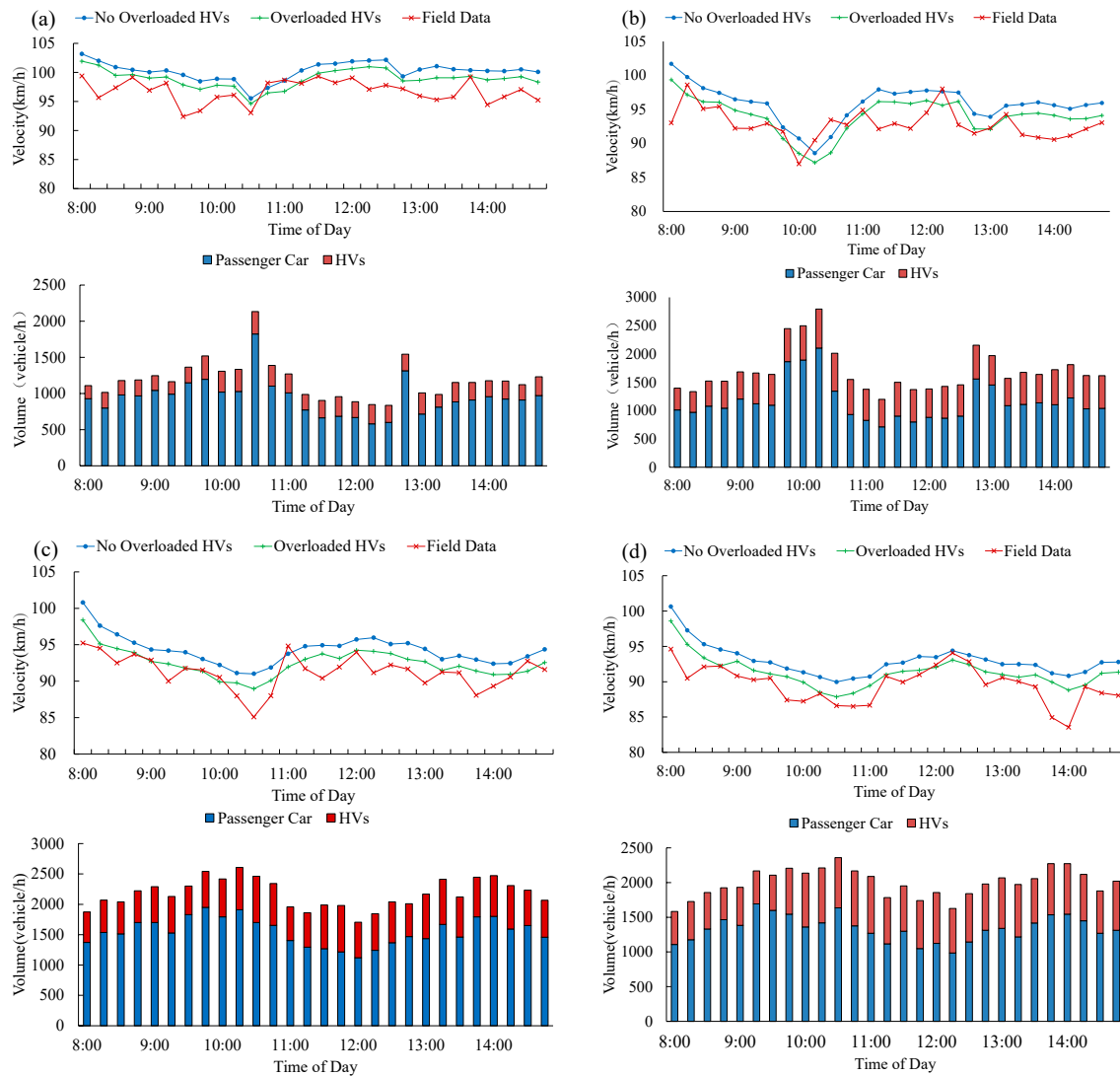


Figure 3. Comparison of passenger car travel speed from model results and field data on (a) Sunday; 1 July 2012; (b) Monday, 2 July 2012; (c) Wednesday, 4 July 2012; and (d) Friday, 27 July 2012.

Mean absolute percentage error (MAPE) was used to evaluate the accuracy of the model results (Table 6):

$$MAPE = \frac{100\%}{n_T} \sum_{i=1}^{n_T} \left| \frac{V_{M(i)} - V_{A(i)}}{V_{A(i)}} \right| \tag{18}$$

where $V_{M(i)}$ is the model result of travel speed during time interval i , $V_{A(i)}$ is the actual travel speed during time interval i , and n_T is the number of time intervals.

Table 6. Characteristics of traffic demand and the MAPE of model results.

| Date | Average Volume (Vehicle/h) | | | | | Overloading Proportion of HVs (%) | MAPE | | | |
|---------|----------------------------|-----|-----|-----|-----|-----------------------------------|-------|-------------------|----------------|----------------|
| | PC1 | HV1 | HV2 | HV3 | HV4 | | HV5 | No Overloaded HVs | Overloaded HVs | MAPE Reduction |
| 1 July | 883 | 47 | 70 | 48 | 28 | 48 | 16.2% | 3.78% | 2.08% | 45.0% |
| 2 July | 1083 | 114 | 199 | 81 | 47 | 101 | 13.9% | 3.66% | 2.50% | 31.7% |
| 4 July | 1195 | 118 | 186 | 113 | 71 | 114 | 17.3% | 3.34% | 1.72% | 48.5% |
| 27 July | 1251 | 119 | 205 | 118 | 55 | 160 | 15.8% | 3.58% | 2.38% | 33.5% |

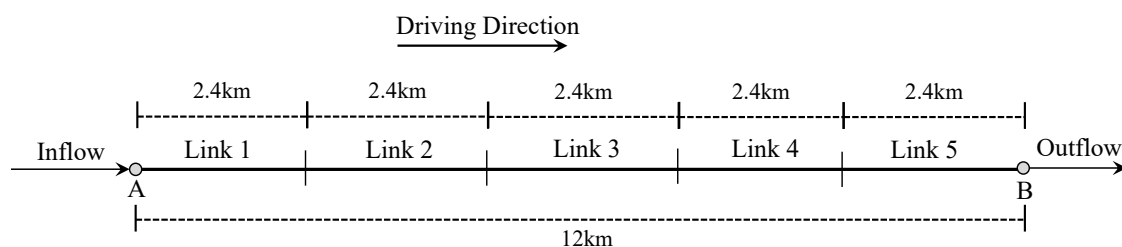
It can be found that the MAPE improved when there were overloaded HVs. The reduction of MAPE was more than 30% during the four testing days. When the overloading proportion of HVs was higher, the reduction of MAPE was more significant. The results show that the proposed model can represent the traffic conditions more realistically when considering for overloaded HVs. When the overloading performance is serious, the traffic condition will be overrated by traditional models that treat overloaded HVs as normal ones, and this will lead to heavy traffic congestion in reality. Thus, the freeway traffic managers cannot evaluate the accurate traffic condition, which may lead to inappropriate traffic management strategies. In China, the freeway toll data include vehicle type, vehicle weight, total weight limit, etc., which provides the data fundamental for the proposed model on practical application. However, there are still some time intervals suffering a relatively large gap, although the model results fit the field data for the overall trend. This is mainly caused by the factors affecting the traffic conditions that have not been considered in the proposed model, e.g., the lane-changing behavior of different vehicles, weather condition, and other stochastic disturbances. All of these will lead to the deviation, and improvements can be considered in further studies.

Moreover, to analyze the impact of overloaded HVs on traffic conditions in different demand and supply combinations, several scenario tests were conducted and are discussed in Section 6.

6. Model Scenario Test

6.1. Preparation of the Scenario Test

To identify the impacts of overloaded HVs on traffic conditions, a simple freeway segment type without merge/diverge was chosen in this simulation test. The freeway basic segment is 12 km with two lanes. It is split evenly into five links, and each link is 2.4 km long. All the vehicles entered the freeway segment from station A, and then left from station B (Figure 4). The analysis time interval was 1 min and the total time period was 30 min. The freeway segment was empty at initial status. Only PC1 and HV5 were represented in this scenario test, and all the parameters were the same as in Table 4.

**Figure 4.** Test a single freeway segment.

6.2. Scenario 1: Impact of the Overloading Proportion

Scenario 1 aims to exhibit the impact of overloaded HVs when the overloading proportion (i.e., the number of overloaded HVs/ the total number of HVs) changes. The flow rate of passenger cars was 3500 veh/h for the entire testing time period. The inflow rate of HVs was 1500 veh/h during

the first 10 min, then this dropped to zero immediately, and the overloading ratio was fixed as 25%. The only changing variable was the overloading proportion, which ranges from 0 to 40%. The speed variation of PC1 on link 1 is shown in Figure 5.

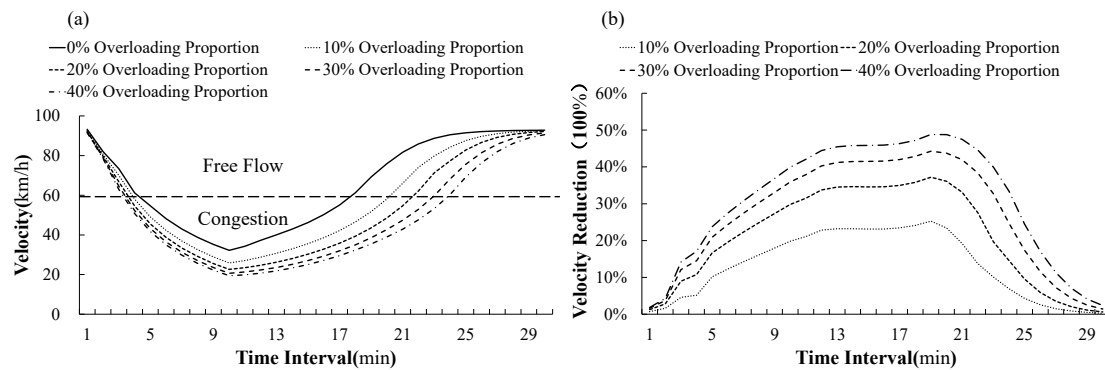


Figure 5. (a) Speed with different overloading proportions on link 1. (b) Speed reduction with different overloading proportions on link 1.

As seen in Figure 5, passenger car speeds decreased with increasing overloading proportions. Compared with the situation when there was no overloaded HV, the maximum speed reduction ratio was 48.8% when the overloading proportion was 40%. Meanwhile, when the overloading proportion was higher, the duration of congestion was longer. For instance, the length of the congestion period was 19 or 23 min when the overloading proportion was 10 or 40%, respectively.

It is also noticeable in Figure 5b that the first 10% of overloaded HVs brought the most negative impacts. The maximum speed reduction was 25.3% when the overloaded proportion was 10%. However, when the overloaded proportion increased to 20%, the maximum speed reduction was 37.2%. This is less than 50.6% (i.e., the double of 25.3%), meaning that although the total impacts increased with increasing overloaded proportions, the average impact of each overloaded HV decreased. This is consistent with Highway Capacity Manual (HCM 2010) [5] that “when there are more HVs on a freeway, the HVs could form platoons and have less interaction with passenger cars”.

6.3. Scenario 2: Impact of the Overloaded HVs at Work Zones

Scenario 2 aims to represent the impact of overloaded HVs on traffic conditions around work zones. A work zone located on link 3 caused one lane closure from the 11th minute to the 15th minute, i.e., the capacity of link 3 reduced by half. The flow rates of passenger cars and HVs were both fixed throughout the entire time period at 2000 and 1000 veh/h, respectively. In this scenario, the only changing variable is the overloading proportion, and the overloading ratio is fixed as 25%. The traffic flow propagation method is discussed in Appendix B. The speed variation of PC1 is shown in Figure 6.

As seen in Figure 6a, when one lane was closed and no overloaded vehicle exists, link 3 suffered from capacity reduction and the speed of passenger cars decreased at first. Meanwhile, link 2 suffered from a lower outflow rate due to the capacity reduction of link 3. The inflow of link 4 and link 5 became smaller, therefore, their traffic conditions were better. When the closed lane on link 3 opened again at the 16th minute, the residual vehicles on link 2 entered link 3 with a larger inflow rate, so link 3 still suffered from poor traffic conditions, although its capacity recovered. These vehicles kept driving through the downstream links and led to worsen traffic conditions on link 4 and link 5 after the closed lane opened.

As seen in Figure 6b–d, the congestion became more serious when the overloading proportion increased, especially on link 2 and link 3. Compared with the situation without overloaded HVs, the lowest speed on link 2 and link 3 decreased 24.7 and 6.5%, respectively, and the low speed duration under 80 km/h on link 2 and link 3 increased 98 and 51%, respectively, when the overloading proportion was 40%. It can be found that the travel speeds of all vehicles were lower when there were

more overloaded HVs. Additionally, it took more time for the overloaded HVs to drive through the work zone, and they caused a longer congestion duration. Meanwhile, there were more overloaded HVs stocked on link 2 due to the capacity reduction on link 3, when the proportion of overloaded HVs increased. This explains why link 2 suffered from the largest speed reduction.

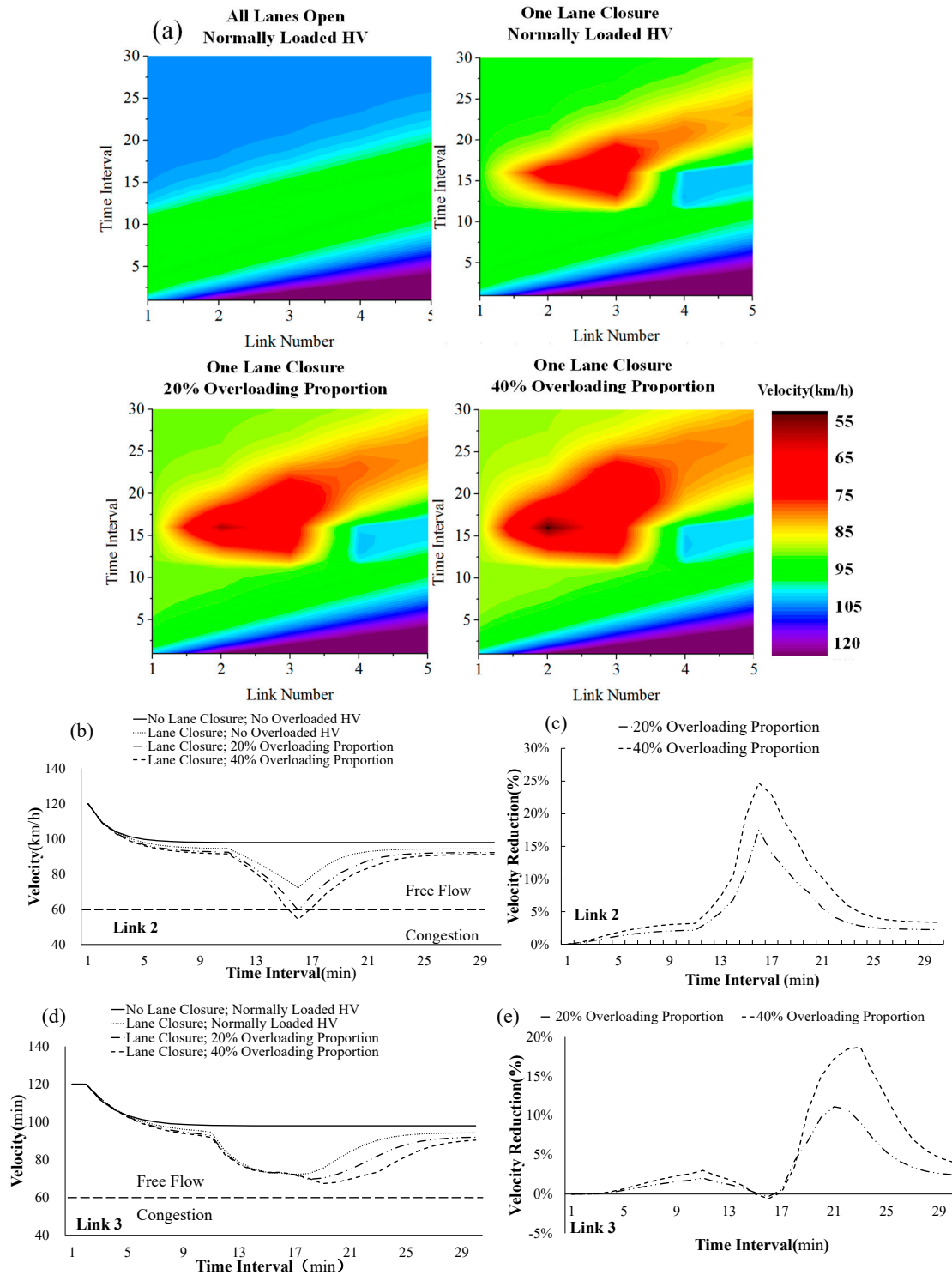


Figure 6. (a) Speed variations on both spatial and temporal dimensions. (b) Speed on link 2. (c) Speed reduction on link 2. (d) Speed on link 3. (e) Speed reduction on link 3.

6.4. Policy Suggestions

The results of the above two scenarios show that the congestion level becomes worse and congestion duration increases with the overloading proportions. This indicates that the existing overloaded HVs do not only cause pavement damage but also lead to low travel speed and an inferior level of service, especially when capacity drop (i.e., work zone) exists. Therefore, it is recommended that overloaded HVs should be forbidden, and the penalty of overloaded HVs should both consider pavement damage and traffic condition influences.

7. Conclusions and Recommendations

Overloaded HVs impose significant impacts on traffic conditions due to their inferior driving performance. However, few existing analytical tools properly address the impact of overloaded HVs on a large-scale network for the online application. In this study, the relationship between overloading ratio and travel speed of overloaded HVs has been analyzed using field data. A new dynamic PCE based on space occupancy was designed for the overloaded HVs, and it can represent the different influences of overloaded HVs when the traffic condition changes. Finally, a new multi-class kinematic wave traffic flow model based on dynamic PCE and the Smulders fundamental diagram was proposed with considerations for the existence of overloaded HVs. Meanwhile, the existence and uniqueness of effective density and the effective volume of the proposed multi-class traffic flow model was proven.

The results of the proposed model are valid. The empirical study shows the model can represent actual traffic conditions, and the model is more accurate with considerations for the existence of overloaded HVs. The improvements in accuracy increase when there are more overloaded HVs. Moreover, the results of scenario tests are plausible, and they show that the increase of the overloading proportion leads to larger speed reductions and longer congestion durations. The proposed model can be used for the online estimation of freeway traffic conditions with considerations for overloaded HVs. It also can help authorities determine traffic management strategies accordingly.

However, there are several improvements that could be implemented in further studies. First, a multi-level model instead of several separate models for each HV type may be more appropriate on the regression between maximum speed and overloading ratio. Meanwhile, the proposed model can be extended to a multi-lane version to describe vehicle interaction during lane changing. Moreover, the dynamic PCE includes the proportion of HVs and a fixed adjustment parameter is used. Other functions could be made to represent the relationship between PCE and vehicle type proportion better. Furthermore, the space occupancy function could be improved by incorporating other advanced car-following models. Additionally, how to obtain and update the multi-class traffic flow parameters with different environmental conditions will be a future study direction.

Author Contributions: All authors contributed to the research presented in this paper. Conceptualization: X.W.; methodology: X.W.; formal analysis: X.W. and Y.T.; data curation: X.W. and P.Z.; writing—original draft preparation: X.W. and P.Z.; writing—review and editing: X.W., Y.T., and P.Z.; funding acquisition: X.W.

Funding: The Natural Science Foundation of Jiangsu Province under grant no. BK20160324 and the Natural Science Foundation of Jiangsu Colleges and Universities under grant no. 16KJB580009 supported this work.

Acknowledgments: The authors are grateful to the Jiangsu Freeway Network Operation and Management Center for providing the necessary freeway toll data used in this study. Computational support was provided by the School of Rail Transportation, Soochow University.

Conflicts of Interest: The authors declare no conflict of interest.

Nomenclature

| | |
|---------------|--|
| F_u | the maximum braking force of vehicle type u |
| L_u | the length of vehicle type u |
| $N_{u,i}$ | the number of vehicle type u on link i |
| $N_{1,i}$ | the number of passenger cars on link i |
| $N_{(i,j)}^p$ | the data size from toll station i to j after data quality control in time period p |

| | |
|------------------|--|
| $Q_{in(u,i)}^k$ | the number of vehicles of class u arriving on link i during time interval k |
| $Q_{out(u,i)}^k$ | the number of vehicles of class u leaving from link i during time interval k |
| S_u | the stopping distance of normal HVs |
| S_u^r | the stopping distance of overloaded HVs |
| $T_{u,i}$ | the headway of vehicle type u on link i |
| $T_{(i,j)}^p$ | the travel time from entry station i to exit station j in time period p |
| $V_M(i)$ | the model result of travel speed during time interval i |
| $V_A(i)$ | the actual travel speed during time interval i |
| m_u | the total weight of normal HVs |
| m_u^r | the total weight of overloaded HVs |
| n_T | the number of time intervals |
| $p_{u,i}$ | the proportion of vehicle type u against the total number of passenger cars and vehicle type u |
| r | the overloading ratio |
| $t_{en(k)}^p$ | the entry time of vehicle k entering during time period p |
| $t_{ex(k)}^p$ | the exit time of vehicle k |
| $t_{on(i)}^p$ | the travel time along the on-ramp of entry station i |
| $t_{off(j)}^p$ | the travel time along the off-ramp of exit station j |
| v_u | the speed of vehicle type u |
| $v_{u,max}$ | the maximum speed of vehicle type u |
| $v_{u,max}^r$ | the maximum speed of vehicle type u when the overloading ratio is r |
| v_u^r | the travel speed of overloaded HVs |
| v_{crit} | the critical speed |
| w | the shockwave speed |
| x_i | the length of link i |
| α | the adjustment ratio of the HV proportion |
| $\eta_{u,i}$ | the dynamic PCE of vehicle type u on link i |
| $\rho_{u,i}^k$ | the density of vehicle type u on link i during time interval k |
| ρ_e | the effective density |
| ρ_{crit} | the critical density |
| ρ_{jam} | the jam density |

Appendix A. The Solution of Effective Density

The solution of effective density is mainly based on the workflow that van Wageningen-Kessels proposed [24,25], with necessary modifications.

Appendix A.1. Transformation of Effective Density

To find one uniform formula of effective density for both free flow and congestion regimes, some parameterizations need to be done. The uniform formula will be used to solve effective density.

In free-flow, set $a_u^f = L_u + T_u v_{u,max}$ and $b_u^f = -T_u \frac{v_{u,max} - v_{crit}}{\rho_{crit}}$.

In congestion, set $a_u^c = T_u w \rho_{jam}$ and $b_u^c = L_u - T_u w$.

According to Equations (3), (4), (6), and (14), the effective density of free flow and congestion can be rewritten as:

$$\rho_e = \sum_u f(p_u) \cdot \frac{a_u + b_u \rho_e}{a_1 + b_1 \rho_e} \cdot \rho_u \quad (A1)$$

Appendix A.2. Requirements on Parameters

1. Speed

It is reasonable to assume that the small passenger car (i.e., PC1) has the highest maximum speed among all vehicle types, and the maximum speeds of all vehicle types should not be lower than the critical speed:

$$v_{\text{crit}} \leq v_{u,\text{max}} \leq v_{1,\text{max}} \quad (\text{A2})$$

In free flow, the effective volume should increase with the effective density, which implicates that $dq_e/d\rho_e > 0$. Assume there are only passenger cars in free flow, and

$$dq_e/d\rho_e = v_{1,\text{max}} - 2 \frac{v_{1,\text{max}} - v_{\text{crit}}}{\rho_{\text{crit}}} \rho_e \geq 0 \quad (\text{A3})$$

When $\rho_e = \rho_{\text{crit}}$, Equation (A3) becomes

$$v_{1,\text{max}} - 2 \frac{v_{1,\text{max}} - v_{\text{crit}}}{\rho_{\text{crit}}} \rho_{\text{crit}} \geq 0 \Rightarrow v_{1,\text{max}} \leq 2v_{\text{crit}} \quad (\text{A4})$$

In conclusion, the maximum speeds are bounded by

$$v_{\text{crit}} \leq v_{u,\text{max}} \leq v_{1,\text{max}} \leq 2v_{\text{crit}} \quad (\text{A5})$$

2. Headway

Assume there are only passenger cars in congestion. Set the space occupancy of each passenger car as $\omega_1 = v_1 \cdot T_1 + L_1$ and the average available space for each passenger car as $S = 1/\rho_e$. The space occupancy of each vehicle cannot be overlapped, so $\omega_1 \leq S \Rightarrow \omega_1 - S \leq 0$. When combining this with Equation (4) and $\rho_{\text{jam}} = 1/L_1$, the above inequality becomes:

$$\omega_1 - S = L_1 + T_1 \cdot w \left(\frac{S}{L_1} - 1 \right) - S = (L_1 - S) \frac{L_1 - T_1 w}{L_1} \leq 0 \quad (\text{A6})$$

Since $L_1 < S$, it requires that $L_1 - T_1 w \geq 0$.

Assume the number of vehicle type u and passenger car as fixed values under congestion. Another new vehicle type, u' , joins the traffic flow and causes the increase of effective density. In this more congested situation, the dynamic PCE of vehicle type u should not decrease, which means $d\eta_u/d\rho_e > 0$.

Based on Equations (4) and (6) and $v_u = v_1$ in congestion, $d\eta_u/d\rho_e$ is equal to:

$$d\eta_u/d\rho_e = f(p_u) \cdot \frac{L_1 T_u - L_u T_1}{(L_1 + T_1 v_1)^2} \cdot \frac{dv_u}{d\rho_e} \geq 0 \quad (\text{A7})$$

According to Equation (4), $\frac{dv_u}{d\rho_e} = -w \frac{\rho_{\text{jam}}}{\rho_e^2} \leq 0$. This requires $L_1 T_u - L_u T_1 \leq 0$ to be true.

In conclusion, the requirements on space occupancy are:

$$\frac{T_u}{L_u} \leq \frac{T_1}{L_1} \leq \frac{1}{w} \quad (\text{A8})$$

Appendix A.3. Solution of Effective Density

Multiplying $a_1 + b_1 \rho_e$ on both sides, Equation (A1) can be changed to a quadratic function:

$$a_1 \rho_e + b_1 \rho_e^2 = \sum_u f(p_u) \rho_u a_u + \sum_u f(p_u) \rho_u b_u \rho_e \quad (\text{A9})$$

By setting $c_u = \sum_u f(p_u) \rho_u a_u$, Equation (26) can be rewritten as:

$$b_1 \rho_e^2 + (a_1 - \sum_u f(p_u) \rho_u b_u) \rho_e - c_u = 0 \quad (\text{A10})$$

The two roots of the quadratic function are:

$$\rho_e = \begin{cases} \frac{(-a_1 + \sum_u f(p_u)\rho_u b_u) + \sqrt{(a_1 - \sum_u f(p_u)\rho_u b_u)^2 + 4b_1 c_u}}{2b_1} \\ \frac{(-a_1 + \sum_u f(p_u)\rho_u b_u) - \sqrt{(a_1 - \sum_u f(p_u)\rho_u b_u)^2 + 4b_1 c_u}}{2b_1} \end{cases} \quad (\text{A11})$$

In order to get effective density, the existence of a solution in Equation (A11) needs to be proven, and the correct root should be chosen.

Set $B = a_1 - \sum_u f(p_u)\rho_u b_u$ and $D = B^2 + 4b_1 c_u$.

1. Existence of Solution

B can be transformed into the following:

$$\begin{aligned} B &= a_1 - \sum_u f(p_u)\rho_u b_u - \frac{\sum_u f(p_u)a_u \rho_u}{\rho_e} + \frac{\sum_u f(p_u)a_u \rho_u}{\rho_e} \\ &= a_1 - \frac{a_1 + b_1 \rho_e}{\rho_e} \sum_u f(p_u)\rho_u \frac{a_u + b_u \rho_e}{a_1 + b_1 \rho_e} + \frac{\sum_u f(p_u)a_u \rho_u}{\rho_e} \end{aligned} \quad (\text{A12})$$

Put Equation (A1) into Equation (A12) to replace $\sum_u f(p_u)\rho_u \frac{a_u + b_u \rho_e}{a_1 + b_1 \rho_e}$ with ρ_e , and then Equation (A12) is rewritten as:

$$B = a_1 - \frac{a_1 + b_1 \rho_e}{\rho_e} \rho_e + \frac{\sum_u f(p_u)a_u \rho_u}{\rho_e} = \frac{\sum_u f(p_u)a_u \rho_u}{\rho_e} - b_1 \rho_e \quad (\text{A13})$$

Combining $c_u = \sum_u f(p_u)\rho_u a_u$ and Equation (A13), $D = B^2 + 4b_1 c_u$ can be transformed into

$$\begin{aligned} D &= \left(\frac{\sum_u f(p_u)a_u \rho_u}{\rho_e} \right)^2 + (b_1 \rho_e)^2 - 2b_1 \sum_u f(p_u)a_u \rho_u + 4b_1 \sum_u f(p_u)\rho_u a_u \\ &= \left(\frac{\sum_u f(p_u)a_u \rho_u}{\rho_e} + b_1 \rho_e \right)^2 \geq 0 \end{aligned} \quad (\text{A14})$$

Because $D \geq 0$, Equation (A11) has real roots.

2. Choice of the Correct Root

Based on Equation (A14), effective density can be rewritten as:

$$\rho_e = \begin{cases} \frac{(-a_1 + \sum_u f(p_u)\rho_u b_u) + \left| \frac{\sum_u f(p_u)a_u \rho_u}{\rho_e} + b_1 \rho_e \right|}{2b_1} \\ \frac{(-a_1 + \sum_u f(p_u)\rho_u b_u) - \left| \frac{\sum_u f(p_u)a_u \rho_u}{\rho_e} + b_1 \rho_e \right|}{2b_1} \end{cases} \quad (\text{A15})$$

Combining this with Equation (A13), $B + 2b_1^c \rho_e$ can be rewritten as:

$$B + 2b_1^c \rho_e = \frac{\sum_u f(p_u)a_u^c \rho_u}{\rho_e} + b_1^c \rho_e \quad (\text{A16})$$

(1) Free-Flow

Combining $B = a_1 - \sum_u f(p_u)\rho_u b_u$, $a_u^f = L_u + T_u v_{u,\max}$ and $b_u^f = -T_u \frac{v_{u,\max} - v_{\text{crit}}}{\rho_{\text{crit}}}$, $B + 2b_1^f \rho_e$ can be rewritten as:

$$B + 2b^f_1\rho_e = a^f_1 + 2b^f_1\rho_e - \sum_u f(p_u)\rho_u b^f_u \tag{A17}$$

Since $b^f_u = -T_u \frac{v_{u,max} - v_{crit}}{\rho_{crit}} \leq 0$, $f(p_u)\rho_u \geq 0 \Rightarrow \sum_u f(p_u)\rho_u b^f_u \leq 0$

Meanwhile, considering that $\rho_e \leq \rho_{crit}$ and $v_{1,max} \leq 2v_{crit}$ (i.e., (A4)), it can be proven that

$$\begin{aligned} a^f_1 + 2b^f_1\rho_e &\geq a^f_1 + 2b^f_1\rho_{crit} = L_1 + T_1v_{1,max} - 2T_1(v_{1,max} - v_{crit}) \\ &= L_1 + T_1(2v_{crit} - v_{1,max}) \geq 0 \end{aligned} \tag{A18}$$

Then:

$$B + 2b^f_1\rho_e = a^f_1 + 2b^f_1\rho_e - \sum_u f(p_u)\rho_u b^f_u \geq 0 \tag{A19}$$

(2) Congestion

Since $a^c_u = T_u w \rho_{jam} > 0$ and $b^c_1 = L_1 - T_1 w \geq 0$ (i.e., (A8)), it can be proven that:

$$\frac{\sum_u f(p_u) a^c_u \rho_u}{\rho_e} \geq 0, b^c_1 \rho_e \geq 0 \Rightarrow B + 2b^c_1 \rho_e \geq 0 \tag{A20}$$

In conclusion, the first root in Equation (A15), $\rho_e = \frac{-B + |B + 2b^c_1 \rho_e|}{2b^c_1} = \frac{-B + B + 2b^c_1 \rho_e}{2b^c_1} = \rho_e$, is the right root no matter whether the situation is in free flow or congestion, and the first root in Equation (A11) can be used.

Appendix B. The Solution of the Density for Each Vehicle Type

The density of vehicle type u can be calculated using Equation (A21) as shown below:

$$\rho^k_{u,i} = \frac{Q^k_{in(u,i)} - Q^k_{out(u,i)}}{x_i} + \rho^{k-1}_{u,i} \tag{A21}$$

where $\rho^k_{u,i}$ is the density of vehicle type u on link i at time interval k , x_i is the length of link i , $Q^k_{in(u,i)}$ is the number of vehicles of class u arriving on link i at time interval k , and $Q^k_{out(u,i)}$ is the number of vehicles of class u leaving from link i at time interval k .

The calculation of $Q^k_{in(u,i)}$ and $Q^k_{out(u,i)}$ is based on the minimum supply and demand method [26] when there are on-ramps or off-ramps between link i and link $i + 1$. This study just focuses on the impact of overloaded HVs on the mainline section, so it assumes there is no on-ramp or off-ramp between link i and $i + 1$, and the direction of traffic flow is from link i to link $i + 1$. The entering vehicle number of link $i + 1$ should be equal to the exiting vehicle number of link i :

$$Q^k_{in(u,i+1)} = Q^k_{out(u,i)} \tag{A22}$$

$Q^k_{out(u,i)}$ can be represented using Equation (A22):

$$Q^k_{out(u,i)} = \frac{1}{\eta^{k-1}_{u,i}} \min(D^{k-1}_{u,i}, S^{k-1}_{u,i+1}) \cdot \Delta t \tag{A23}$$

$$D^{k-1}_{u,i} = \begin{cases} q^{k-1}_{e(u,i)} \rho^{k-1}_{e(i)} < \rho_{crit(i)} \\ \lambda^{k-1}_{u,i} \cdot q_{crit(i)} \rho^{k-1}_{e(i)} \geq \rho_{crit(i)} \end{cases}; S^{k-1}_{u,i+1} = \begin{cases} \lambda^{k-1}_{u,i} \cdot q_{crit(i+1)} \rho^{k-1}_{e(i+1)} < \rho_{crit(i+1)} \\ q^{k-1}_{e(u,i+1)} \rho^{k-1}_{e(i+1)} \geq \rho_{crit(i+1)} \end{cases} \tag{A24}$$

$$\lambda^{k-1}_{u,i} = \frac{q^{k-1}_{e(u,i)}}{\sum_u q^{k-1}_{e(u,i)}} \tag{A25}$$

where $\eta_{u,i}^{k-1}$ is the dynamic PCE of vehicle type u on link i during time interval $k - 1$, $D_{u,i}^{k-1}$ is the demand of vehicle type u on link i during time interval $k - 1$, $S_{u,i+1}^{k-1}$ is the supply of vehicle type u on link $i + 1$ during time interval $k - 1$, $q_{e(u,i)}^{k-1}$ is the effective volume of vehicle type u on link $i + 1$ during time interval $k - 1$, $q_{\text{crit}(i)}$ is the critical volume of link I , $\rho_{e(i)}^{k-1}$ is the effective density on link i at time interval $k - 1$, $\rho_{\text{crit}(i)}$ is the critical density of link I , and $\lambda_{u,i}^{k-1}$ is the effective proportion of vehicle type u on link i during time interval $k - 1$.

References

- Ren, Y.; Wu, S. Analysis of heavy trucks' effect on freeway traffic safety. In Proceedings of the 2011 International Conference on Electronic and Mechanical Engineering and Information Technology (EMEIT), Harbin, China, 12–14 August 2011.
- Xiao, R.; Li, B.; Chen, Y. Trend analysis of expressway transportation based on big data. *J. Traffic Transp. Eng.* **2015**, *117*, 85–90.
- Han, W.; Wu, J.; Cai, C.S.; Chen, S. Characteristics and dynamic impact of overloaded extra heavy trucks on typical highway bridges. *J. Bridge Eng.* **2014**, *20*, 05014011. [[CrossRef](#)]
- Zhou, H.W.; Li, G.X.; Shi, K.T. *Jiangsu Freeway Traffic Condition Analyzing Report*; Jiangsu Freeway Network Operation & Management Center: Nanjing, China, 2012.
- Manual, H.C. HCM2010. In *Transportation Research Board*; National Research Council: Washington, DC, USA, 2010.
- Aghabayk, K.; Sarvi, M.; Young, W. A macroscopic study of heavy vehicle traffic flow characteristics. In Proceedings of the ARRB Conference, Perth, Australia, 23–26 September 2012.
- Aghabayk, K.; Sarvi, M.; Young, W. Understanding the dynamics of heavy vehicle interactions in car-following. *J. Transp. Eng.* **2012**, *138*, 1468–1475. [[CrossRef](#)]
- Abdullah, A.S. *Development of Integrated Weigh-in-Motion System and Analysis of Traffic Flow Characteristics considering Vehicle Weight*; The University of Tokushima Japan: Tokushima, Japan, 2011.
- Saifizul, A.A.; Yamanaka, H.; Karim, M.R. Empirical analysis of gross vehicle weight and free flow speed and consideration on its relation with differential speed limit. *Acc. Anal. Prev.* **2011**, *43*, 1068–1073. [[CrossRef](#)] [[PubMed](#)]
- Dhamaniya, A.; Chandra, S. Concept of Stream Equivalency Factor for Heterogeneous Traffic on Urban Arterial Roads. *J. Transp. Eng.* **2013**, *139*, 1117–1123. [[CrossRef](#)]
- Cao, N.Y.; Sano, K. Estimating capacity and motorcycle equivalent units on urban roads in Hanoi, Vietnam. *J. Transp. Eng.* **2012**, *138*, 776–785. [[CrossRef](#)]
- Geistefeldt, J. Estimation of passenger car equivalents based on capacity variability. *Transp. Res. Rec.* **2009**, *2130*, 1–6. [[CrossRef](#)]
- De Luca, M.; Dell'Acqua, G. Calibrating the passenger car equivalent on Italian two line highways: A case study. *Transport* **2013**, *29*, 1–8.
- Ahmed, U.; Drakopoulos, A.; Ng, M. Impact of Heavy Vehicles on Freeway Operating Characteristics under Congested Conditions. *Transp. Res. Rec.* **2013**, *2396*, 28–37. [[CrossRef](#)]
- Mehar, A.; Chandra, S.; Velmurugan, S. Passenger Car Units at Different Levels of Service for Capacity Analysis of Multilane Interurban Highways in India. *J. Transp. Eng.* **2013**, *140*, 81–88. [[CrossRef](#)]
- van Lint, J.W.C.; Hoogendoorn, S.P.; Schreuder, M. Fastlane: New Multiclass First-Order Traffic Flow Model. *Transp. Res. Rec.* **2008**, *2088*, 177–187. [[CrossRef](#)]
- Ngoduy, D. Multiclass first-order traffic model using stochastic fundamental diagrams. *Transportmetrica* **2011**, *7*, 111–125. [[CrossRef](#)]
- Bellomo, N.; Dogbe, C. On the modeling of traffic and crowds: A survey of models, speculations, and perspectives. *SIAM Rev.* **2011**, *53*, 409–463. [[CrossRef](#)]
- Logghe, S.; Immers, L.H. Multi-class kinematic wave theory of traffic flow. *Transp. Res. Part B Methodol.* **2008**, *42*, 523–541. [[CrossRef](#)]
- Del Castillo, J.M. Three new models for the flow–density relationship: Derivation and testing for freeway and urban data. *Transportmetrica* **2012**, *8*, 443–465. [[CrossRef](#)]

21. Daganzo, C.F. A behavioral theory of multi-lane traffic flow. Part I: Long homogeneous freeway sections. *Transp. Res. Part B Methodol.* **2002**, *36*, 131–158. [[CrossRef](#)]
22. Chanut, S.; Buisson, C. Macroscopic model and its numerical solution for two-flow mixed traffic with different speeds and lengths. *Transp. Res. Rec.* **2003**, *1852*, 209–219. [[CrossRef](#)]
23. Ngoduy, D.; Liu, R. Multiclass first-order simulation model to explain non-linear traffic phenomena. *Phys. A Stat. Mech. Appl.* **2007**, *385*, 667–682. [[CrossRef](#)]
24. Van Wageningen-Kessels, F.; Van Lint, H.; Hoogendoorn, S.; Vuik, K. A New Generic Multi-class Kinematic Wave Traffic Flow Model: Model Development and Analysis of Its Properties. *Transportation* **2014**, *29*, 449–456.
25. Van Wageningen-Kessels, F. Multi-Class Continuum Traffic Flow Models: Analysis and Simulation methods. Ph.D. Thesis, Delft University of Technology/TRAIL Research School, Delft, The Netherlands, 2013.
26. Wang, X.; Chen, X. Travel time estimation of a single segment based on freeway toll data. In Proceedings of the 14th COTA International Conference of Transportation Professionals: Safe, Smart, and Sustainable Multimodal Transportation Systems, CICTP 2014, Changsha, China, 4–7 July 2014; pp. 2161–2174.
27. Smulders, S. Control of freeway traffic flow by variable speed signs. *Transp. Res. Part B Methodol.* **1990**, *24*, 111–132. [[CrossRef](#)]
28. Qu, X.; Zhang, J.; Wang, S. On the stochastic fundamental diagram for freeway traffic: model development, analytical properties, validation, and extensive applications. *Transp. Res. Part B Methodol.* **2017**, *104*, 256–271. [[CrossRef](#)]
29. Daganzo, C.F. The cell transmission model: A dynamic representation of highway traffic consistent with the hydrodynamic theory. *Transp. Res. Part B Methodol.* **1994**, *28*, 269–287. [[CrossRef](#)]
30. Qu, X.; Wang, S.; Zhang, J. On the fundamental diagram for freeway traffic: A novel calibration approach for single-regime models. *Transp. Res. Part B Methodol.* **2015**, *73*, 91–102. [[CrossRef](#)]
31. Yang, D.; Jin, P.; Pu, Y.; Ran, B. Safe distance car-following model including backward-looking and its stability analysis. *Eur. Phys. J. B* **2013**, *86*, 92. [[CrossRef](#)]
32. Marlina, S. *Understanding the Dynamics of Truck Traffic on Freeways by Evaluating Truck Passenger Car Equivalent (PCE) in the Highway Capacity Manual (HCM) 2010*; University of Colorado at Denver: Denver, CO, USA, 2012.



© 2018 by the authors. Licensee MDPI, Basel, Switzerland. This article is an open access article distributed under the terms and conditions of the Creative Commons Attribution (CC BY) license (<http://creativecommons.org/licenses/by/4.0/>).